Molecular Pharmacology Fast Forward. Published on January 23, 2007 as doi:10.1124/mol.106.031286

Methylmercury-Induced Increase of Intracellular Ca^{2+} Increases Spontaneous Synaptic Current Frequency in Rat Cerebellar Slices

Yukun Yuan and William D. Atchison
Department of Pharmacology/Toxicology
Michigan State University, East Lansing, MI 48824, USA

RUNNING TITLE PAGE

Running Title: Disruption of cerebellar synaptic function by methylmercury

Address all correspondences including reprint requests to:
William D. Atchison, Ph.D.
Department of Pharmacology/Toxicology
B331 Life Sciences Building
Michigan State University
East Lansing, MI 48824-1317, USA

Phone: (517) 353-4947
Fax: (517) 432-1341
Email: atchiso1@msu.edu

# of text pages:	24
# of figures	8
# of tables	1
# of words in abstract	236
# of words in introduction	473
# of words in discussion	2273

Abbreviations:

ACSF- artificial cerebrospinal fluid; APV- amino-5-phosphonopentanoic acid; ANOVA- analyses of variance; $[Ca^{2+}]_i$- intracellular calcium concentration; CNQX- 6-Cyano-7-nitroquinoxaline-2,3-dione; EPSC- excitatory postsynaptic current; EPSP- excitatory postsynaptic potential; IPSC- inhibitory postsynaptic current; MeHg- methylmercury; mEPSP- miniature excitatory postsynaptic potential; mIPSP- miniature inhibitory postsynaptic potential; ROI- region of interest; sEPSC- spontaneous excitatory postsynaptic current; sIPSC- spontaneous inhibitory postsynaptic current

Molecular Pharmacology Fast Forward. Published on January 23, 2007 as DOI: 10.1124/mol.106.031286
This article has not been copyedited and formatted. The final version may differ from this version.

ABSTRACT

The relationship between increased intracellular calcium concentration-$[Ca^{2+}]_i$ and changes in spontaneous synaptic current frequency caused by the neurotoxicant methylmercury (MeHg) was examined in Purkinje cells of cerebellar slices using confocal microscopy and whole-cell recording. MeHg (10-100 μM) stimulated and then suppressed completely the frequency of spontaneous postsynaptic currents (sEPSCs and sIPSCs). Current amplitude was also initially increased. The same MeHg concentrations increased markedly fluorescence of the Ca^{2+} indicator Fluo-4 throughout the molecular layer as well as the granule cells. No changes in fluorescence occurred in Purkinje cell soma, although fluorescence increased in their subplasmalemmal shell. Simultaneous confocal imaging and whole-cell recording revealed that time to onset of MeHg-induced increase in fluorescence in the molecular layer correlated with that of increased sEPSC and sIPSC frequency in Purkinje cells. Pretreatment with the intracellular Ca^{2+} chelator BAPTA significantly suppressed the MeHg-induced increase in sIPSC frequency, further suggesting that MeHg-induced elevation of $[Ca^{2+}]_i$ is partially responsible for its early stimulatory effects on spontaneous synaptic responses. However when spontaneous synaptic currents ceased with MeHg, Fluo-4 fluorescence remained elevated. Thus synaptic transmission cessation is apparently not related to changes in $[Ca^{2+}]_i$. It may result from effects of MeHg on transmitter release or sensitivity of postsynaptic receptors. The lack of effect of MeHg on Purkinje cell somal fluorescence reinforces that they are more resistant to MeHg-induced elevations of $[Ca^{2+}]_i$ than other cells, including cerebellar granule cells.

Molecular Pharmacology Fast Forward. Published on January 23, 2007 as DOI: 10.1124/mol.106.031286
This article has not been copyedited and formatted. The final version may differ from this version.

INTRODUCTION

Acute and chronic exposure to methylmercury (MeHg), a potent environmental neurotoxicant, causes a series of severe neurological disorders which include disruption of motor functions (Hunter and Russell, 1954; Takeuchi et al., 1968; Bakir et al., 1973; Chang, 1977). Effects of MeHg poisoning are especially pronounced on the cerebellar cortex, which is also a sensitive target of MeHg *in vitro*. The exact mechanisms underlying MeHg-induced neurological dysfunction remain unclear. However, disruption by MeHg of synaptic function is likely to contribute to these effects because MeHg interferes with synaptic transmission in isolated systems by both presynaptic and postsynaptic effects (See Atchison and Hare, 1994; Limke et al., 2004; Atchison, 2003; 2005 for review).

A common feature of the effects of MeHg *in vitro* on synaptic transmission is an initial increase followed by a decrease in spontaneous release of neurotransmitter. For example, *in vitro* bath application of MeHg caused initial stimulation prior to suppression of the frequency and amplitude of $GABA_A$ receptor-mediated spontaneous and miniature inhibitory postsynaptic currents (sIPSCs and mIPSCs) in granule and particularly Purkinje cells in cerebellar slices (Yuan and Atchison, 2003, 2005). This pattern of effects of MeHg on synaptic transmission, particularly on the frequency of spontaneous synaptic events, appears to be universal, regardless of whether the synapse is of peripheral or central origin, or excitatory or inhibitory in nature. It also occurs after *in vivo* treatment of animals with MeHg. Juang and Yonemura (1975) reported an initial increase in frequency of miniature excitatory postsynaptic potentials (mEPSPs) in sympathetic ganglia in guinea pigs following MeHg exposure. These results suggest that a

Molecular Pharmacology Fast Forward. Published on January 23, 2007 as DOI: 10.1124/mol.106.031286
This article has not been copyedited and formatted. The final version may differ from this version.

common mechanism underlies the presynaptic effects of MeHg on asynchronous release of neurotransmitter.

The rate of spontaneous or asynchronous release of neurotransmitter from presynaptic terminals is associated with increased $[Ca^{2+}]_i$ but is not necessarily dependent on function of voltage-gated Ca^{2+} channels. MeHg increases $[Ca^{2+}]_i$ in a number of cell types in primary culture including cerebellar granule and Purkinje cells (Hare et al., 1993; Marty and Atchison, 1997; Edwards et al., 2005), albeit with differing sensitivity. Thus, it is reasonable to link the initial stimulatory effects of MeHg on synaptic transmission to the MeHg-induced increase in $[Ca^{2+}]_i$ in the presynaptic terminals. However, this correlation has never been demonstrated. Furthermore, it is unclear what is responsible for the secondary decrease in neurotransmitter release and whether $[Ca^{2+}]_i$ remains elevated at that time.

The present study was designed specifically to examine the relationship between MeHg-induced changes in $[Ca^{2+}]_i$ and frequency of spontaneous synaptic responses in Purkinje cells in cerebellar slices. More specifically, we sought to determine if MeHg-induced elevation of $[Ca^{2+}]_i$ in presynaptic terminals is correlated temporally and spatially to MeHg-induced initial increases in frequency of spontaneous synaptic responses in Purkinje cells. A combination of confocal imaging of $[Ca^{2+}]_i$ and whole-cell patch-clamp recordings of spontaneous synaptic currents in Purkinje cells in freshly isolated cerebellar slices, was used to compare the time courses of effects of MeHg on $[Ca^{2+}]_i$ in the presynaptic fibers and those on frequency of sIPSCs or spontaneous excitatory postsynaptic currents (sEPSCs) recorded from the soma of Purkinje cells.

Molecular Pharmacology Fast Forward. Published on January 23, 2007 as DOI: 10.1124/mol.106.031286
This article has not been copyedited and formatted. The final version may differ from this version.

MATERIAL AND METHODS

Chemicals. Methylmercuric chloride, purchased from ICN Biomedical, Inc (Costa, CA), was dissolved in deionized water to a final concentration of 10 mM to serve as stock solution. The applied solutions (10 - 100 μM) were diluted with artificial cerebrospinal fluid (ACSF) just before perfusion. Three MeHg concentrations (10 μM, 20 μM and 100 μM) were used in the present study. The rationale for use of these concentrations of MeHg has been detailed elsewhere (Yuan and Atchison, 2003, 2005). Fluo-4 acetoxymethyl ester (AM) (Fluo-4/AM) and 1,2 bis(2-aminophenoxy)ethane-*N*,*N*,*N*',*N*'-tetra-acetic acid acetoxymethyl ester (BAPTA/AM) were purchased from Molecular Probes, (Eugene, OR). Pluronic F-127, 6-cyano-7-nitroquinoxaline-2,3-dione (CNQX), amino-5-phosphonopentanoic acid (APV) and (-)-bicuculline methobromide were all purchased from Sigma Chemical Co. (St Louis, MO).

Preparation of cerebellar slices. All animal procedures complied with the National Institutes of Health of the USA guidelines on animal care and were approved by Michigan State University Institutional Animal Use and Care Committee. Cerebellar slices were prepared as described previously (Yuan and Atchison, 1999; 2003), using Sprague-Dawley rats (10 - 21 days postnatal, either gender) (Harlan Industries, Verona, WI). The "slicing" solution contained (in mM): 125, NaCl; 2.5, KCl; 4, $MgCl_2$; 1.25, KH_2PO_4; 26, $NaHCO_3$; 1, $CaCl_2$ and 20, D-glucose (pH 7.35 - 7.4 when saturated with 95% O_2 /5% CO_2 at room temperature of 22 - 25^oC). ACSF, in which all experiments were conducted, consisted of (in mM): 125, NaCl; 2.5, KCl; 1, $MgCl_2$;

1.25, KH_2PO_4; 26, $NaHCO_3$; 2, $CaCl_2$ and 25, D-glucose (pH 7.35 - 7.4 saturated with 95% O_2 /5% CO_2 at room temperature).

Whole cell recording in cerebellar slices. Recording methods were detailed in Yuan and Atchison (2003, 2005). Purkinje cells in slices were identified based on their characteristic electrophysiological properties and visually by their size, shape and location using a Nikon E600FN upright microscope (Nikon Optics, Tokyo, Japan) equipped with Nomarski optics (x 40 water immersion objective) and Sony IR-1000 infrared CCD video camera system (DAGE MTI, Michigan City, IN). Recording electrodes coated with Sylgard resin 184 (Dow Corning, Midland, MI) and fire-polished, had resistances of 2 - 4 MΩ when filled. The pipette solution consisted of (in mM): 140, CsCl; 4, NaCl; 0.5, $CaCl_2$; 10, HEPES; 5, EGTA, 2, Mg-ATP and 0.4, GTP (pH 7.3 adjusted with CsOH) for recording sIPSCs, or 140, K-gluconate; 4, NaCl; 0.5, $CaCl_2$; 10, HEPES; 5, EGTA, 2, Mg-ATP and 0.4, GTP (pH 7.3 adjusted with KOH) for recording sEPSCs. Whole cell recordings of sIPSCs or sEPSCs were made using standard "blow and seal" techniques (Stuart et al., 1993). The holding potential was -60 mV for sIPSCs and -70 mV for sEPSCs. CNQX, (10 μM) and APV, (50 - 100 μM) were added to the external solution to block glutamate receptor-mediated sEPSCs. Bicuculline (10 μM) was added to block $GABA_A$ receptor-mediated sIPSCs. Data acquisition was as described in Yuan and Atchison (2003). Whole cell currents were filtered at 2 - 5 kHz with an 8-pole low-pass Bessel filter and digitized at 10 - 20 kHz for later off-line analysis using pClamp8.1 or 9.0 program (Axon Instruments, Union City, CA). All experiments were carried out at room temperature of 22 - 25 ºC. Only one

slice per rat was used for any given experiment and only one concentration of MeHg was applied per slice.

Data analysis was as described in Yuan and Atchison (2003). In brief, spontaneous synaptic currents were first screened automatically using MiniAnalysis software (Synaptosoft Inc., Decatur, GA) with a set of the prespecified parameters. They were then accepted or rejected manually with an event detection amplitude threshold at 5 pA for sEPSCs and 10 pA for sIPSs, and based on the kinetic properties (fast rising phase and slow decay phase) of the spontaneous events. Unless specified otherwise, at least 100 events per cell over a 2 min period were averaged to calculate the frequency of spontaneous synaptic currents. Peak amplitudes of currents were measured at the absolute maximum after subtraction of the baseline noise.

Confocal fluorescence microscopy. Cerebellar slices were loaded for 40 - 60 min at room temperature with 4 μM Fluo-4/AM in the presence of 0.02% (w v^{-1}) pluronic F-127. Slices were then washed thoroughly with ACSF. Confocal images of Fluo-4 fluorescence ($[Ca^{2+}]_i$) in cerebellar slices were obtained using a Leica TCS SL laser scanning microscope system (Leica Microsystem, Heifelberg GmbH., Germany) equipped with Nomarski optics (x 40 water immersion objective, n.a, 0.75). Fluo-4 fluorescence was excited by 488 nm light from an argon laser attenuated to 20% with neutral density. Emitted fluorescence was collected at >515 nm. Images (512 x 512 pixels, xyz or xyt scan mode) were collected before and during exposure to 10, 20 or 100 μM MeHg. In experiments in which simultaneous changes were examined in both sIPSCs in Purkinje cells and Fluo-4 fluorescence in the molecular layer, Purkinje cells and granule cell layers in a given cerebellar slice, whole-cell recordings of sIPSCs were made in

Molecular Pharmacology Fast Forward. Published on January 23, 2007 as DOI: 10.1124/mol.106.031286
This article has not been copyedited and formatted. The final version may differ from this version.

Purkinje cells in cerebellar slices preloaded with Fluo-4. After establishment of the whole-cell recording configuration, both sIPSCs and Fluo-4 fluorescence were recorded continuously in the absence and presence of MeHg. To avoid photobleaching of Fluo-4, sensitivity was adjusted to a minimal level.

Changes in Fluo-4 fluorescence intensity in a given cerebellar cortical layer were analyzed using Leica software. Data from several regions of interests (ROIs) defined within this layer were averaged. The background Fluo-4 fluorescence was subtracted from all ROIs before averaging.

Statistical analysis. Data were analyzed statistically using Student's paired *t* test or one-way analysis of variance (ANOVA) for MeHg concentration- or time-dependent measures, unless otherwise specified. Dunnett's procedure was used for *post hoc* comparisons (Tukey-Kramer multiple comparison test). Differences between two cumulative amplitude or inter-event distribution curves obtained before and after exposure to MeHg at a given time were compared using, the Komogorov-Smirnov test. Values were considered statistically significant at $p \leq 0.05$. The data are presented as mean ± standard error of the mean (SEM). Each experiment was replicated in a minimum of five slices; the actual number of replicates for each experiment is listed in the corresponding figure legend.

RESULTS

MeHg causes biphasic changes in frequency of both sEPSCs and sIPSCs.

Effects of MeHg on glutamatergic synaptic transmission were examined as changes in frequency and amplitude of Purkinje cell sEPSCs. Shown in Figure 1 is a representative recording of effects of MeHg on sEPSCs. Prior to exposure to MeHg (Fig. 1*A*), the mean frequency and amplitude of sEPSCs over a 2 min recording episode in the Purkinje cell in this sagittal cerebellar slice were 0.9 Hz and 21.3 pA (112 events), respectively. Bicuculline was present to block $GABA_A$ receptor-mediated sIPSCs. Continuous bath application of 20 μM MeHg to this slice gradually increased both frequency and amplitude of sEPSCs. After 25 min of MeHg exposure, the mean frequency and amplitude were increased to 21.9 Hz and 33.9 pA (2636 events), respectively. Subsequently, whereas the sEPSC frequency continued to increase, the amplitude began to decrease. sEPSC frequency was eventually reduced after 60 min and sEPSCs disappeared completely after 70 min of MeHg exposure (data not shown). Figure 1*H* specifically demonstrates the MeHg-induced initial effect on sEPSC frequency. It is expressed as changes in inter-sEPSC intervals during the first 25 min of MeHg exposure. MeHg significantly reduced the inter-sEPSC interval and shifted the curves to the left ($p < 0.05$, Kolmogorov-Smirnov test), indicating an increase in frequency of sEPSCs.

Similar biphasic changes in frequency and amplitude were also seen in slices exposed to 10 or 100 μM MeHg. After exposure of slices to 10 μM or 100 μM MeHg, respectively, both sEPSC frequency and amplitude were initially increased prominently prior to complete cessation (data not shown). Figure 2*A* specifically demonstrates time courses of effects of these MeHg concentrations on sEPSC frequency. In consideration of the variation among individual

experiments, and to permit a direct comparison, all data of sEPSC frequency obtained during MeHg exposure are normalized to the pre-MeHg treatment control value. At 100 μM, MeHg both stimulated and then suppressed sEPSC frequency rapidly. Peak sEPSC frequency was initially increased almost 10x higher than that of the control ($p < 0.05$, Student's paired *t* test). It then began to decline to complete cessation after 20 min of MeHg exposure. Times to peak increases in frequency of sEPSCs were inversely related to MeHg concentrations tested, reflecting the differences in time course. The mean times to peak increases of sEPSC frequency for 10, 20 and 100 μM MeHg were 37.5 ± 4.8 min (n = 6), 24.6 ± 4.0 min (n = 13) and 6.7 ± 0.8 min (n = 11), respectively. These differences are statistically significant (ANOVA, $p < 0.05$). However, the percentages of peak increase induced by the three MeHg concentrations are not statistically significant (ANOVA, $p > 0.05$). As with the times to peak increases in sEPSC frequency, time to complete block of sEPSCs was also MeHg concentration-dependent. Thus, the generalized effect of MeHg on glutamatergic sEPSCs is biphasic, concentration- and time-dependent.

We have previously shown that bath application of MeHg caused a similar biphasic effect on GABAergic sIPSCs or mIPSCs in Purkinje cells in cerebellar slices (Yuan and Atchison, 2003, 2005). To compare the relative effectiveness of MeHg on excitatory and inhibitory transmission, we re-examined the effect of MeHg on Purkinje cell sIPSCs under similar conditions to those used for sEPSC recordings. As observed previously, MeHg also initially stimulated and then decreased both the frequency and amplitude of sIPSCs. Figure 2*B* shows time-courses of effects for the three MeHg concentrations on sIPSC frequency. Values were again normalized to pretreatment control. At 100 μM MeHg sIPSC frequency increased

Molecular Pharmacology Fast Forward. Published on January 23, 2007 as DOI: 10.1124/mol.106.031286
This article has not been copyedited and formatted. The final version may differ from this version.

rapidly (12.1 ± 2.3 Hz, n = 10) by almost 3x the control (from 4.8 ± 1.4 Hz) $p < 0.05$, Student's paired *t* test). At 20 and 10 μM MeHg, sIPSC frequency increased from pretreatment values of 3.9 ± 0.8 or 3.1 ± 0.9 Hz to peak responses of 11.0 ± 1.4 (n = 12) or 8.2 ± 1.4 Hz (n = 5), respectively. But as with the effects on sEPSCs, the time courses were relatively slower compared with those obtained at 100 μM MeHg. Differences among times to onset of peak increase and block of sIPSC induced by different MeHg concentrations are statistically significant (ANOVA, $p < 0.05$), although the percentages of peak increase in sIPSC frequencies induced by the three MeHg concentrations are not (ANOVA, $p > 0.05$).

The next goal was to determine the reversibility of MeHg-induced initial increase in sIPSC frequency and the effects of two successive applications of MeHg on sIPSCs. In this set of experiments, slices were treated twice with MeHg in succession. They were first exposed to either 20 or 100 μM MeHg following a stable control baseline recording. Once a marked increase of sIPSC frequency occurred, slices were washed immediately with MeHg-free ACSF. Washing for 5 - 15 min initially stabilized the sIPSC frequency and then gradually restored it at or near the pre-MeHg treatment levels (data not shown). Some cells fired repetitively in the presence of MeHg; washing also effectively stopped such firing (data not shown). After sIPSC frequency became stable, the response of this cell to a second exposure to the same concentration of MeHg was recorded. As described for the effects of a single application of MeHg (Fig 2*B*), the second application of MeHg initially increased sIPSC frequency then gradually suppressed it to complete cessation of sIPSCs (data not shown). An identical pattern of effects was observed in six slices prepared from three rats following exposure to either 20 or

Molecular Pharmacology Fast Forward. Published on January 23, 2007 as DOI: 10.1124/mol.106.031286
This article has not been copyedited and formatted. The final version may differ from this version.

100 μM MeHg. These results suggest that the early stimulatory effects of MeHg on sIPSC frequency are reversible.

Table 1 compares the mean times to onset of MeHg-induced peak increase and complete block of sEPSCs or sIPSCs. The times to peak increase of sEPSC and sIPSC frequency and block are similar. Although it took slightly longer for MeHg, particularly at low concentrations, to block sEPSCs than it did sIPSCs, the difference between times to complete block of sEPSCs and sIPSCs were not statistically significant ($p > 0.05$). Thus, the pattern of effects of MeHg on glutamatergic and GABAergic spontaneous currents is similar.

MeHg induced an increase in $[Ca^{2+}]_i$ in molecular and granule cell layers, but not Purkinje cell soma in cerebellar slices.

Although spontaneous, asynchronous release is independent of depolarization-induced influx of Ca^{2+} into nerve terminals, its frequency is directly proportional to the free $[Ca^{2+}]_i$ (Llinás and Nicholson, 1975; Otis and Mody, 1992; Savič and Sciancalepore, 1998). The MeHg-induced early stimulatory effects on frequency of spontaneous synaptic currents might be due to MeHg-induced increases in presynaptic $[Ca^{2+}]_i$. To test this, we compared the temporal and spatial changes in $[Ca^{2+}]_i$ in the molecular layer, Purkinje cell layer and granule cell layer of isolated cerebellar slices induced by MeHg. Figure 3 depicts the general pattern and time-course of effect of MeHg on Fluo-4 fluorescence intensity as expressed in pseudocolor changes in cerebellar slices. Shown in the top panel are changes in Fluo-4 fluorescence in a representative sagittal slice before (Control) and after various periods of exposure to 10 μM MeHg. All three layers of cerebellar cortex could be clearly identified under low power magnification. The mean

fluorescence intensity in the molecular layer averaged from several ROIs after subtraction of background fluorescence is 41.89 intensity $Pixel^{-1}$ prior to MeHg exposure. Application of MeHg caused a gradual increase in fluorescence throughout the molecular layer including individual interneurons. By 40 - 60 min after beginning MeHg, mean fluorescence intensity was increased to 131 - 167% of pretreatment control. Fluorescence intensity in the granule cell layer also increased markedly. By 40 min after MeHg exposure, mean fluorescence in the cells was 252% of control. While fluorescence in the dendrites of Purkinje cells was also increased by MeHg, that in the soma of Purkinje cells did not appear to be affected.

Parallel fibers in the molecular layer run perpendicular to the planar Purkinje cell dendrites, and thus are truncated in sagittal slices. Consequently, to obtain a more accurate view of MeHg-induced changes in $[Ca^{2+}]_i$ in glutamate-secreting parallel fibers, transverse or coronal cerebellar slices were used in the next set of experiments. As shown for the transverse slice in Figure 3 (Bottom panel), MeHg (20 μM) also increased markedly fluorescence in the molecular and granule cell layer. Fluorescence was particularly strong (shown as blue color) at the outer region of the molecular layer, where the parallel fibers travel and synapse with the dendritic trees of Purkinje cells and interneurons. At 25 min after beginning MeHg, fluorescence intensity was increased to ~ 360% of pretreatment control. Similar results were seen in slices exposed to 10 or 100 μM MeHg (data not shown). Thus, the $[Ca^{2+}]_i$ in parallel fibers is also elevated by MeHg exposure, an effect consistent with that in the granule cell bodies. In addition, the time courses of MeHg-induced increases in fluorescence in both the molecular and granule cell layers in transverse cerebellar slices are similar to those in sagittal slices.

Figure 4 (Top) specifically shows the effect of MeHg (100 μM) on Purkinje cell dendrites in another sagittal slice. Fluorescence increased 2 min after exposure of this slice to MeHg (data not shown); it peaked at 8 - 15 min. Subsequently, fluorescence began to diminish after 20 min (data not shown). The time course of increases in fluorescence intensity appears to be very similar to that of effects of MeHg on the frequency and amplitude of sEPSCs or sIPSCs recorded from Purkinje cells (Figs. 1 and 2).

The lack of effect of MeHg on Fluo-4 fluorescence in the Purkinje cell soma is shown more clearly in another slice exposed to 20 μM MeHg for 30 min in Figure 4 (Bottom). Conversely fluorescence apparently increased in the subplasmalemmal shell (as indicated by the arrows) 20 min after MeHg exposure (Fig. 4, Bottom). This failure of MeHg to increase Fluo-4 fluorescence in Purkinje cell soma was a consistent observation seen in all cerebellar slices examined. Thus, MeHg apparently increased $[Ca^{2+}]_i$ of granule cells, dendrites of Purkinje cells and those presynaptic fibers which synapse with Purkinje cells, but not Purkinje cell soma.

MeHg-induced increase in presynaptic $[Ca^{2+}]_i$ and sIPSC frequency in Purkinje cells coincides.

We next specifically analyzed the time courses of effects of MeHg on Fluo-4 fluorescence intensity in the molecular and granule cell layers. As shown in Figure 5*A*, at 20 μM MeHg, fluorescence intensity in both layers was increased markedly. By 20 min of MeHg exposure, fluorescence was increased to 180 ± 32% and 149 ± 5% of pretreatment controls in the molecular and granule cell layers, respectively (n = 8). In Figure 5*B*, the mean time to onset of maximum increase in Fluo-4 fluorescence in the molecular layer was compared specifically to

Molecular Pharmacology Fast Forward. Published on January 23, 2007 as DOI: 10.1124/mol.106.031286
This article has not been copyedited and formatted. The final version may differ from this version.

onset of peak increase in frequency of sIPSCs in Purkinje cells. Time to maximum Fluo-4 fluorescence (21.9 ± 4.1 min) was virtually identical to that for peak sEPSC frequency (24.6 ± 4.0 min, $p > 0.05$, n = 13) or sIPSC frequency (20.0 ± 2.2 min, $p > 0.05$, n = 12). However, unlike the effect of 20 μM MeHg on frequency of sEPSCs or sIPSCs, which started to decline rapidly after 40 min of MeHg exposure and was blocked almost completely at 60 min (Fig. 2*A* and 2*B*), Fluo-4 fluorescence remained relatively elevated at 122 ± 41% and 91 ± 20% of the controls, respectively, in the molecular and granule cell layers after 60 min of MeHg exposure. Thus, at the time at which EPSCs, or sIPSCs were blocked completely, $[Ca^{2+}]_i$ remains higher than or approximately equal to that prior to MeHg exposure. A similar pattern of changes in Fluo-4 fluorescence in the cell layers was also seen after exposure to 100 μM MeHg (Fig. 5*C*), but it took relatively longer to reach the maximum increase in Fluo-4 fluorescence (13.25 ± 1.11 min, n = 9) than it did to induce the peak increase in sEPSC frequency (6.7 ± 0.8 min, n = 11) or sIPSC frequency (6.8 ± 0.5 min, n = 10). This suggests that the increase in $[Ca^{2+}]_i$ is an ongoing and continuous process, which is beyond the level required for maximum release of neurotransmitter.

Inasmuch as the electrophysiological recordings and confocal fluorescence microscopy described above were done separately and exhibited variability in the time courses of increased $[Ca^{2+}]_i$ across slices, it was possible that the two responses merely coincided. Therefore, we next combined the two techniques to examine simultaneously the effects of MeHg on sIPSCS and temporal and spatial changes in $[Ca^{2+}]_i$ in a given individual slice. We recorded sIPSCs instead of sEPSCs in this set of experiments because the frequency of occurrence of sIPSCs in Purkinje cells is higher and the amplitude larger than those of sEPSCs. Consequently, they were easier to

record when symmetric [Cl^-] conditions are applied. Figure 6 depicts a representative example of such an experiment. Changes in Fluo-4 fluorescence signal were monitored throughout the whole molecular layer in the absence and presence of 20 μM MeHg. At the same time, changes in sIPSC frequency in a Purkinje cell in that slice were recorded continuously before and during MeHg exposure. When fluorescence intensity in the molecular layer began to increase at 15 min after MeHg exposure, the frequency of sIPSCs also increased dramatically. However, after sIPSC frequency declined significantly at 50 min and sIPSCs disappeared completely at 60 min after MeHg exposure, Fluo-4 fluorescence remained strong. In another example, Figure 7 specifically shows the relationship between changes in sIPSC frequency and Fluo-4 fluorescence in both molecular and granule cell layers. In this slice, sIPSC frequency was increased prominently at 2 - 4 min after exposure to 100 μM MeHg and disappeared almost completely after 12 min. In contrast, changes in Fluo-4 fluorescence intensity were relatively slow. Apparent changes in Fluo-4 fluorescence could only be seen after 8 min of MeHg exposure (data not shown). After 16 min of MeHg exposure, both the granule cell and molecular layer, including dendrites of Purkinje cells, showed a pronounced increase in Fluo-4 fluorescence. Again, the increased fluorescence remained strong at the time at which sIPSCs were completely blocked. These data suggest that either presynaptic neurotransmitter release was affected or sensitivity of postsynaptic receptors to neurotransmitter was altered by MeHg, although $[Ca^{2+}]_i$ in the presynaptic terminals might remain high.

If MeHg-induced elevation of $[Ca^{2+}]_i$ in presynaptic fibers or neurons is indeed responsible for the initial changes in frequency of spontaneous synaptic events, prevention of such increases in $[Ca^{2+}]_i$ should block or at least reduce or delay MeHg-induced initial changes

Molecular Pharmacology Fast Forward. Published on January 23, 2007 as DOI: 10.1124/mol.106.031286
This article has not been copyedited and formatted. The final version may differ from this version.

in spontaneous transmitter release. Thus, the final set of experiments was designed specifically to test this using an Ca^{2+}_i chelator. Slices were first incubated with 50 μM BAPTA/AM, a membrane-permeant Ca^{2+}_i chelator, for 30 min, then followed by superfusion with solution containing 20 or 100 μM MeHg plus 50 μM BAPTA/AM. Shown in Figure 8*A*-*H* is a representative example of time course of effect of 20 μM MeHg on Purkinje cell sIPSC frequency in the presence of BAPTA. Prior to BAPTA treatment (Fig. 8*A*), the frequency and amplitude of sIPSCs in this cell were 8.9 Hz and 74.1 pA (averaged from 1072 events over a 2-min recording episode), respectively. After incubation with BAPTA for 30 min, both sIPSC frequency and amplitude were reduced markedly (Fig. 8*B*). The mean frequency and amplitude of sIPSCs were 53% and 52% of control (from 12.7 ± 2.8 Hz and 141.8 ± 33.2 pA to 7.6 ± 2.2 Hz and 56.5 ± 8.2 pA, n = 14), respectively. However, exposure of the slice to MeHg (for 25 min in this case) still caused a partial recovery of sIPSC frequency (Fig. 8*E*) prior to its eventual disappearance (Fig. 8*H*). To a greater or lesser extent, all six slices tested showed an initial, transient recovery of sIPSC frequency during MeHg exposure in the presence of BAPTA. Figure 8*I* compares time-courses of effects of 20 and 100 μM MeHg on Purkinje cells sIPSC frequency in the presence of BAPTA. All data were normalized to the pre-BAPTA (at -30 min) values. MeHg exposure began at 0 min in the continuous presence of BAPTA. At 20 μM, MeHg again caused a small rebound increase (i.e. 151 ± 43%, n = 7) prior to a gradual suppression of sIPSC frequency. However, sIPSC frequency never recovered completely to the values of pre-BAPTA treatment control (at -30 min). Compared with the initial increase in sIPSC frequency induced by 20 μM MeHg in the absence of BAPTA treatment (Fig. 2*B*), these data clearly demonstrate that BAPTA treatment effectively suppressed the initial increase in

Molecular Pharmacology Fast Forward. Published on January 23, 2007 as DOI: 10.1124/mol.106.031286
This article has not been copyedited and formatted. The final version may differ from this version.

sIPSC frequency induced by MeHg. In contrast, 100 μM MeHg induced a much more pronounced initial increase in sIPSC frequency even in the continuous presence of BAPTA. sIPSC frequency increased to 305 ± 102% of the values of pre-MeHg treatment after 30 min BAPTA incubation (at 0 min) or 160 ± 56% of pre-BAPTA treatment control (at -30 min). Compared with the initial increase in sIPSC frequency induced by the same concentration of MeHg in the absence of BAPTA pretreatment (almost 300% of control at 100 μM shown in Fig. 2*B*), however, the effect on sIPSC frequency in the presence of BAPTA never reached the same levels of increase as it did in its absence. Although BAPTA may have been applied at an insufficient concentration, it was still able to suppress partially the initial increase of sIPSC frequency induced by higher concentrations of MeHg. The mean times to onset of peak increase (relative to the values of pre-MeHg treatment at 0 min) in sIPSC frequency induced by 20 and 100 μM MeHg in the presence of BAPTA were 23.6 ± 5.6 (n = 6) and 5.6 ± 0.5 min (n = 7), respectively. These were similar to those obtained in the absence of BAPTA (Fig. 2*B* and Table 1). However, neither MeHg concentration was able to increase the amplitudes of sIPSCs significantly in the presence of BAPTA (data not shown). Thus, these data clearly demonstrate that Ca^{2+}_i chelation reduces the levels of MeHg-induced initial stimulation of spontaneous transmitter release although it did not appear to delay significantly the onset of MeHg-induced initial stimulatory effects. Somehow, increasing $[Ca^{2+}]_i$ by MeHg also contributes to the effects of MeHg on sIPSC amplitude.

DISCUSSION

The primary goal of the present study was to determine if MeHg-induced elevation of $[Ca^{2+}]_i$ in the presynaptic fibers that make synaptic contacts with Purkinje cells is correlated to the initial stimulatory effects of MeHg on frequency of spontaneous synaptic currents. To this end, effects of MeHg on spontaneous postsynaptic responses and the temporal and spatial changes in $[Ca^{2+}]_i$ in the molecular, Purkinje and granule cell layers in acutely isolated cerebellar slices were examined. Both glutamatergic and GABAergic transmission were compared during acute bath application of 10, 20 or 100 μM MeHg, which initially increased then decreased the frequency of sEPSCs or sIPSCs. The maximal increase attained was not concentration-dependent, although the time to onset was inversely correlated with the MeHg concentrations. This initial increase in sIPSC frequency was reversible if washing occurred at the early stage of exposure. Consistent with the initial stimulatory effects of MeHg on sEPSCs and sIPSCs, MeHg also induced prominent increases in Fluo-4 fluorescence intensity in the molecular and granule cell layers, and Purkinje cell dendrites but not somata. Simultaneous examination of MeHg-induced changes in frequency of sIPSCs and Fluo-4 fluorescence in the same cerebellar slice demonstrated that time courses or time to onset of MeHg-induced changes in spontaneous release and $[Ca^{2+}]_i$ were similar. Moreover, pretreatment of slices with BAPTA/AM significantly suppressed MeHg-induced initial increases in frequency and amplitude of sIPSCs.

MeHg-induced initial stimulation of spontaneous release of neurotransmitter from presynaptic nerve terminals is a generalized phenomenon.

Stimulatory effects of MeHg on spontaneous transmitter release were first observed at peripheral synapses such as sympathetic ganglion and neuromuscular junction. In preganglionic fibers of the superior cervical ganglia, both *in vivo* and *in vitro* MeHg treatments caused a significant initial increase in both amplitude and frequency of spontaneous mEPSPs (Juang and Yonemura, 1975). Similarly, *in vitro* MeHg treatment caused a large and transient increase before eventual suppression of frequency of MEPPs at neuromuscular preparations (Juang, 1976, Atchison and Narahashi, 1982). Times to onset of increases in MEPP frequency were approximately 30 - 40 min and 5 - 15 min, respectively, after MeHg exposure to 20 and 100 μM MeHg (Atchison and Narahashi, 1982). The pattern and time courses of effects of MeHg on spontaneous synaptic responses (both sEPSCs and sIPSCs) of Purkinje cells in cerebellar slices in the present study are very similar to those of effects of MeHg on neuromuscular transmission. This suggests that a similar mechanism of action of MeHg occurs on both peripheral and central synapses in terms of spontaneous synaptic responses.

It is generally accepted that changes in frequency of spontaneous synaptic events usually reflect an altered number of quanta of neurotransmitter released (quantal content). Conversely changes in amplitude of postsynaptic responses usually indicate postsynaptic alterations of interactions of transmitter with the receptors, except when the amount of transmitter per vesicle (quantal size) is altered in the presynaptic terminal. At the mammalian neuromuscular junction, it appeared that a primarily presynaptic mechanism was involved in the effects of MeHg on neuromuscular transmission, because after MEPPs were blocked completely by MeHg, iontophoretic application of ACh still induced ACh receptor-mediated postsynaptic responses (Atchison and Narahashi, 1982). Furthermore 40 to 100 μM MeHg had no significant effects on

postsynaptic resting membrane potentials at the neuromuscular junction and peripheral ganglia at the time MEPPs disappeared (Juang and Yonemura, 1975; Juang, 1976; Atchison and Narahashi, 1982). However, the effects of MeHg on central synaptic transmission are more complicated, MeHg could act at multiple sites to block central synaptic transmission in brain slices (Yuan and Atchison, 1993, 1995, 1997, 1999). Thus, both pre- and postsynaptic mechanisms appear to be involved. Alterations of both frequency and amplitudes of sEPSCs and sIPSCs in the present study are consistent with this hypothesis. The MeHg-induced initial increases in the frequency of sEPSCs or sIPSCs are apparently related to an increased presynaptic transmitter release and are consistent with the observations that MeHg stimulated release of several neurotransmitters from rat brain synaptosomes (Minnema et al., 1989). On the other hand, alterations of amplitudes of sEPSCs and sIPSCs are more likely related to effects of MeHg on postsynaptic receptors because MeHg affects responses evoked by iontophoretic application of glutamate or superfusion of the $GABA_A$ receptor agonist muscimol (Yuan and Atchison, 1995, 1997). Thus, these data again suggest that MeHg-induced initial increase in spontaneous neurotransmitter release from presynaptic nerve terminals is a generalized phenomenon and MeHg likely affects spontaneous release through a process that is common to all transmitter systems, irrespective of whether they are peripheral or central in origin, or excitatory or inhibitory in nature.

Time courses of effects of MeHg on sEPSCs and sIPSCs of Purkinje cells in cerebellar slices were generally similar. We previously showed that MeHg blocked evoked IPSPs or IPSCs in CA1 pyramidal neurons in hippocampal slices more rapidly than it did evoked EPSPs or EPSCs (Yuan and Atchison, 1995, 1997). The difference between this and our previous studies may be due to several reasons. 1) Effects of MeHg on synchronous and asynchronous release of

neurotransmitter are different. In fact, it has been shown that spontaneous and evoked synaptic responses in neuromuscular preparations, hippocampal and cerebellar slices all exhibited different temporal sensitivity to MeHg exposure (Atchison and Narahashi, 1982; Yuan and Atchison, 1993, 1999). 2) Differential effects of MeHg on glutamatergic and GABAergic synaptic responses may not be primarily dependent on the type of postsynaptic receptor *per se*, but rather on the types of presynaptic fibers or neurons. In hippocampal CA1 neurons, EPSPs or EPSCs were evoked by subthreshold stimulation of Schaffer collaterals, axons of CA3 pyramidal cells, whereas the recurrent IPSPs or IPSCs were evoked by subthreshold antidromic stimulation of the alveus to activate the interneurons (Yuan and Atchison, 1995, 1997). Small neurons, particularly the GABAergic interneurons in the cerebral cortex, are more sensitive to MeHg-induced neurotoxicity than are pyramidal neurons (O'Kusky, 1985; O'Kusky and McGeer, 1985; O'Kusky et al., 1988; Shigematsu et al., 2000). Thus, in hippocampal CA1 neurons, it is not surprising that IPSPs or IPSCs are more sensitive to block by MeHg than are EPSPs or EPSCs. In cerebellar cortex, both Purkinje cells and interneurons receive glutamatergic inputs from the parallel fibers, the axons of granule cells. The interneurons in turn release GABA onto the dendrites or soma of Purkinje cells. It is well documented that cerebellar granule cells are the most sensitive targets of MeHg in the cerebellar cortex although the stellate interneurons are also highly sensitive to MeHg. Hence, if the differential effects of MeHg on glutamatergic and GABAergic responses reflect a differential action of MeHg on presynaptic neurons or fibers, one should not expect a significantly slower block by MeHg of sEPSCs, particularly those mediated by parallel fibers, as compared with block of sIPSCs. However, Purkinje cells also receive glutamatergic inputs from the climbing fibers. Whether or not the climbing fiber-mediated

Molecular Pharmacology Fast Forward. Published on January 23, 2007 as DOI: 10.1124/mol.106.031286
This article has not been copyedited and formatted. The final version may differ from this version.

sEPSCs are less sensitive to block by MeHg and hence contribute to the slightly longer time courses of effect of MeHg on sEPSCs remains to be determined.

The increased $[Ca^{2+}]_i$ in the presynaptic cells and terminals after MeHg exposure is associated with MeHg-induced increase in frequency of sIPSCs or sEPSCs.

One of the most consistent effects of MeHg *in vitro* is disruption of Ca^{2+} homeostasis leading to increased $[Ca^{2+}]_i$ in a number of cell types including NG108-15 neuroblastoma cells (Hare et al., 1993; Hare and Atchison, 1995), and cerebellar granule and Purkinje cells in culture (Marty and Atchison, 1997, 1998; Limke and Atchison, 2002; Limke et al., 2003; Edwards et al., 2005). MeHg-induced elevations of $[Ca^{2+}]_i$ were also observed in rat brain synaptosomes (Komulainen and Bondy, 1987; Kauppinen et al., 1989; Denny et al., 1993) and non-neuronal cell such as T-lymphocytes (Tan et al., 1993). Thus, this effect too appears to be universal. Because neurotransmitter release from presynaptic terminals is a Ca^{2+}-dependent process, it is likely that MeHg-induced elevation of $[Ca^{2+}]_i$ in the presynaptic terminals contributes to the stimulatory effects of MeHg on frequency of sEPSCs or sIPSCs in Purkinje cells in cerebellar slices. Consistent with this is the observation that increasing $[Ca^{2+}]_o$ or Ca^{2+} permeability at motor nerve terminals shortened the time to onset of MeHg-induced peak increase of MEPP frequency (Atchison, 1986, 1987). Thus, these data imply that MeHg-induced increase in $[Ca^{2+}]_i$ in presynaptic terminals is responsible for the MeHg-induced initial increase in ACh release.

In cerebellar cortex, the molecular layer consists primarily of nerve fibers including parallel fibers formed from axons of granule cells and climbing fibers which originate exclusively from the inferior olive located in the brainstem, dendrites of Purkinje cells and

Molecular Pharmacology Fast Forward. Published on January 23, 2007 as DOI: 10.1124/mol.106.031286
This article has not been copyedited and formatted. The final version may differ from this version.

interneurons (basket and stellate cells). In addition to the two glutamatergic excitatory synaptic inputs, Purkinje cells receive GABAergic inhibitory synaptic inputs from interneuron basket cells and stellate cells. All these fibers in the molecular layer make synapses with the peripheral dendritic tree, proximal dendrites or soma of Purkinje cells. Thus, any changes in Fluo-4 fluorescence signal in the molecular layer should directly reflect changes in $[Ca^{2+}]_i$ in these presynaptic fibers, which in turn should affect release of glutamate or GABA from these presynaptic fibers and hence alter the frequency of spontaneous synaptic currents recorded in the postsynaptic Purkinje cells. Although the confocal Ca^{2+} imaging in the present study did not specifically show changes in $[Ca^{2+}]_i$ at single individual presynaptic fiber level *per se*, the generalized increases in Fluo-4 fluorescence intensity in granule cells and throughout the molecular layers (including interneurons) clearly indicate an increase in $[Ca^{2+}]_i$ in the presynaptic terminals at parallel or climbing fiber-Purkinje cell or interneuron-Purkinje cell synapses after MeHg exposure. The similar time courses, especially the times to onset, of MeHg-induced increases in Fluo-4 fluorescence and frequency of sEPSCs or sIPSCs also clearly suggest that the increased $[Ca^{2+}]_i$ in the presynaptic cells and terminals is associated with MeHg-induced increase in frequency of sEPSCs or sIPSCs.

The soma of Purkinje cells is particularly resistant to MeHg-induced changes in $[Ca^{2+}]_i$.

In addition to the changes in Fluo-4 fluorescence signals in those presynaptic fibers and interneurons in the molecular layer, fluorescence intensity in the major or proximal dendrites was also apparently increased. The increased fluorescence signals in the dendrites of Purkinje cells certainly indicate a postsynaptic change in $[Ca^{2+}]_i$, which might be related to the initial

Molecular Pharmacology Fast Forward. Published on January 23, 2007 as DOI: 10.1124/mol.106.031286
This article has not been copyedited and formatted. The final version may differ from this version.

increase in amplitudes of spontaneous synaptic responses (sEPSCs or sIPSCs) recorded from Purkinje cells after MeHg exposure. The lack of an apparent change in Fluo-4 fluorescence intensity in the soma of Purkinje cells after MeHg exposure is interesting. This spatial nonuniform change in Fluo-4 fluorescence signals in dendrites and the soma of Purkinje cells is consistent with the findings that large and fast Ca^{2+} signals could be found in dendrites but only smaller and slower Ca^{2+} signals can be seen in the soma of Purkinje cells when climbing fibers were activated (Ross and Werman, 1987; Tank et al., 1988; Sugimuri and Llinás, 1990; Miyakawa et al., 1992; Konnerth et al., 1992; Eilers et al., 1995). One explanation provided by Sugimori and Llinás (1990) and Eilers et al. (1995) was that this nonuniform change in Ca^{2+} signals in dendrites and the soma of Purkinje cells in cerebellar slices is due to differential distribution of voltage-gated, particularly P-type, Ca^{2+} channels in dendrites and the soma of mature Purkinje cells-with a low density of Ca^{2+} channels in the somatic region and an abundance particularly in the dendrites (Eilers et al., 1995). Whether or not this is also the case for the differential change in Fluo-4 fluorescence signals in dendrites and the soma of Purkinje cell after MeHg exposure in the present study remains to be determined. However, what is clear is that the Purkinje cell soma is less sensitive to MeHg-induced increase in $[Ca^{2+}]_i$ than is that of granule cells. We have previously shown that Purkinje cells in culture were more resistant to MeHg-induced increase in $[Ca^{2+}]_i$ than were granule cells, even though the two cell types showed a similar pattern of MeHg-induced changes in $[Ca^{2+}]_i$ (Edwards et al., 2005). These results suggest a differential sensitivity of granule and Purkinje cells to MeHg-induced elevation of $[Ca^{2+}]_i$, which may explain why $GABA_A$ receptor-mediated sIPSCs in granule and Purkinje cells demonstrated differential sensitivity to MeHg exposure (Yuan and Atchison, 2003). The reasons

why Purkinje cell soma are more resistant to MeHg-induced increase in $[Ca^{2+}]_i$ remain unclear. Whether or not it is solely related to a differential distribution of Ca^{2+} buffering capacity in addition to a differential distribution of voltage-gated Ca^{2+} channels also remains to be determined.

Fluo-4 fluorescence signals in both molecular and granule cell layers remained very strong when spontaneous synaptic responses were blocked completely by MeHg. These results suggest that either a) neurotransmitter in synaptic vesicles is depleted, b) the release process from presynaptic terminals is blocked, or c) sensitivity of the postsynaptic receptors to neurotransmitter is lost after MeHg exposure. Additionally, cytotoxicity and death of postsynaptic Purkinje cells induced by persistent increases in $[Ca^{2+}]_i$ could play a role in loss of synaptic responses. However, block of spontaneous synaptic responses could not be attributed simply to a nonspecific effect of MeHg-induced cytotoxicity, because our previous studies (Yuan et al., 2005; Yuan and Atchison, 2005) showed that in the same Purkinje cells when sIPSCs disappeared completely, the delayed rectifier-mediated outward K^+ currents and a spontaneous giant inward Cl^- current (possibly mediated by Ca^{2+}-activated Cl^- channels) remained recordable. Similarly, GABA-evoked currents in cerebellar granule cells in culture also appear to be much more sensitive to block by MeHg than are currents mediated by voltage-gated K^+ channels or inwardly rectifying K^+ channels. As noted above, cerebellar granule cells are more sensitive to MeHg-induced cytotoxicity than are Purkinje cells *in vivo* (Leyshon-Sorland et al., 1994) and *in vitro* (Edwards et al., 2005) and sIPSCs in granule cells are 2 - 3 x more sensitive to block by MeHg than are those in Purkinje cells (Yuan and Atchison, 2003). However, in many cases after sIPSCs in granule cells were blocked completely, washing with

Molecular Pharmacology Fast Forward. Published on January 23, 2007 as DOI: 10.1124/mol.106.031286
This article has not been copyedited and formatted. The final version may differ from this version.

MeHg-free solution containing 1 mM D-penicillamine, a MeHg chelator, completely restored the sIPSCs to pre-MeHg treatment level, whereas recovery was not seen in Purkinje cells (Yuan and Atchison, 2003). Moreover, the fact that strong Ca^{2+}_i signals remained after complete block of spontaneous synaptic responses occurred, also suggests that breakdown of membrane integrity is not the primary cause of disappearance of synaptic responses. MeHg-induced cytotoxicity could certainly contribute to later effects of MeHg once spontaneous synaptic responses had ceased. Consistent with this, the eventual reduction in fluorescence signals after extended MeHg exposure might be due to a leak of intracellularly-loaded dye in cells after breakdown of membrane integrity resulting from such MeHg-induced cytotoxicity.

Reduction of MeHg-induced increase in $[Ca^{2+}]_i$ suppresses the early stimulatory effects of MeHg on spontaneous synaptic responses.

Although the time courses of MeHg-induced changes in $[Ca^{2+}]_i$ in presynaptic fibers or neurons and in frequency of spontaneous synaptic events are generally similar, it does not necessarily mean that increased $[Ca^{2+}]_i$ must be directly responsible for the initial changes in frequency of sEPSCs or sIPSCs. Instead, it is still possible that the MeHg-induced increases in frequency of sEPSCs or sIPSCs and changes in Fluo-4 fluorescence or $[Ca^{2+}]_i$ in presynaptic fibers are merely coincidental events. However, significant suppression of MeHg-induced increase, particularly by 20 μM MeHg, in sIPSC frequency in the presence of BAPTA clearly implies that MeHg-induced elevation of $[Ca^{2+}]_i$ is at least partially responsible for the early stimulatory effects of MeHg on spontaneous transmitter release. Although BAPTA-pretreatment was relatively less effective at suppressing the initial increase in sIPSC frequency induced by

Molecular Pharmacology Fast Forward. Published on January 23, 2007 as DOI: 10.1124/mol.106.031286
This article has not been copyedited and formatted. The final version may differ from this version.

100 μM MeHg, the relatively lower percentage of increase in sIPSC frequency (160%) in the presence of BAPTA compared with that (300%) in its absence (Fig. 3*B*) implies that BAPTA did reduce the capacity for a possible maximum increase by MeHg in frequency of sIPSCs by lowering $[Ca^{2+}]_i$. The comparatively lower effectiveness of BAPTA treatment at suppressing 100 μM MeHg-induced initial increase in sIPSC frequency could be due to 1) the BAPTA concentration applied was not sufficient; 2) the increase in $[Ca^{2+}]_i$ caused by 100 μM MeHg was too rapid to be buffered by BAPTA; or 3) MeHg might itself directly stimulate neurotransmitter release. The data that BAPTA pretreatment failed to delay the onset of MeHg-induced initial increase in frequency of sIPSCs might actually support this latter possibility.

In addition to changes in frequency of sIPSCs, MeHg usually also increased sIPSC amplitude initially (Fig. 3*A* and Yuan and Atchison, 2003, 2005). However, in the presence of BAPTA, this effect was markedly suppressed. These data suggest that MeHg-induced elevation of $[Ca^{2+}]_i$ is also involved in postsynaptic effects of MeHg on synaptic responses - a result consistent with the observation that Fluo-4 fluorescence intensity in the dendrites of Purkinje cells was significantly increased (Figs 4, 5, 7, 9 and 10). However the mechanism by which increasing postsynaptic $[Ca^{2+}]_i$ affects sIPSP amplitude is unclear.

The question is how changes in $[Ca^{2+}]_i$ cause the biphasic effect of MeHg on sEPSC or sIPSC frequency. MeHg induces two phases of increase in $[Ca^{2+}]_i$ in several types of cells: an initial low amplitude increase which occurs gradually, followed by a much larger and more rapid increase (Hare et al., 1993; Hare and Atchison, 1995a,b; Marty and Atchison, 1997, 1998; Limke and Atchison, 2002; Limke et al., 2003, 2004). The initial increase in $[Ca^{2+}]_i$ is apparently due primarily to the initial release of Ca^{2+}_i from 1,4,5-iositol triphosphate-sensitive stores in the

smooth endoplasmic reticulum followed by those of mitochondria (Hare and Atchison, 1995; Limke et al., 2003, 2004). The second phase of increase in $[Ca^{2+}]_i$ results from entry of a large amount of extracellular Ca^{2+}. Release of Ca^{2+} from presynaptic internal Ca^{2+} stores contributes to spontaneous transmitter release (see Reviews by Collin et al., 2005 and by Rusakov, 2006). The initial rise of $[Ca^{2+}]_i$ resulting from increased release from internal Ca^{2+} stores in presynaptic terminals facilitates synaptic vesicle docking and fusion at the active zone, and hence increases transmitter release probability. This may be primarily responsible for the MeHg-induced initial increase in sEPSC or sIPSC frequency. Whether or not postsynaptic regulation of presynaptic transmitter by retrograde factors or increased recruitment of postsynaptic receptors are also involved remains unknown. At this stage, the changes in synaptic responses are functional as opposed to structural, and as yet reversible. Consequently washing with MeHg-free solution could reverse the early stimulatory effects. However, persistent increases and overload of $[Ca^{2+}]_i$ will certainly trigger a series of cytotoxic effects leading to cellular dysfunction and eventual cell death. In addition, due partly to its high reactivity with –SH groups and its high lipophilic nature, MeHg itself may directly and indirectly interact with multiple targets including enzymes, receptors and ion channels in cell membranes at both cellular and molecular levels to affect synaptic transmission. These combined effects may be responsible for the late suppression of synaptic responses.

In conclusion, bath application of 10 - 100 μM MeHg induced a prominent increase in $[Ca^{2+}]_i$ in the molecular layer, dendrites of Purkinje cells and granule cell layer of cerebellar slices. The temporal and spatial changes in $[Ca^{2+}]_i$ in the molecular layer are correlated with, or responsible for, the early stimulatory effects of MeHg on spontaneous synaptic responses. The

initial stimulation by MeHg of spontaneous release of neurotransmitter appears to be a generalized phenomenon in MeHg-induced neurotoxic effects *in vitro* on synaptic transmission.

Molecular Pharmacology Fast Forward. Published on January 23, 2007 as DOI: 10.1124/mol.106.031286
This article has not been copyedited and formatted. The final version may differ from this version.

ACKNOWLEDGMENTS

The authors gratefully acknowledge the expert word processing assistance of Erin Koglin and Tara Oeschger, and help with illustrations by Jessica M. Hauptman.

REFERENCES

Atchison WD (1986) Extracellular calcium-dependent and independent effects of methylmercury on spontaneous and potassium-evoked release of acetylcholine at the neuromuscular junction. *J Pharmacol Exp Ther* **237:** 672-680.

Atchison WD (1987) Effects of activation of sodium and calcium entry on spontaneous release of acetylcholine induced by methylmercury. *J Pharmacol Exp Ther* **241:** 131-139.

Atchison WD (2003) Effects of toxic environmental contaminants on voltage-gated calcium channel function: from past to present. *J Bioenerg Biomembr* **35:** 507-532.

Atchison WD (2005) Is chemical neurotransmission altered specifically during methylmercury-induced cerebellar dysfunction? *Trends Pharmacol Sci* **26:**549-557.

Atchison WD and Narahashi T (1982) Methylmercury-induced depression of neuromuscular transmission in the rat. *Neurotoxicology* **3:** 37-50.

Atchison WD and Hare MF (1994) Mechanisms of methylmercury-induced neurotoxicity. *FASEB J* **8:** 622-629.

Bakir F, Damluji S, Amin-Zaki L, Murtadha M, Khalidi A, Al-Rawi NY, Tikriti S, Dahir HI, Clarkson TW, Smith JC and Doherty RA (1973) Methylmercury poisoning in Iraq. *Science* **181:** 230-240.

Chang LW (1977) Neurotoxic effects of mercury--a review. *Environ Res* **14:** 329-373.

Collin T, Marty A and Llano I (2005) Presynaptic calcium stores and synaptic transmission. *Curr Opin Neurobiol* **15**: 275-281.

Denny MF, Hare MF and Atchison WD (1993) Methylmercury alters intrasynaptosomal concentrations of endogenous polyvalent cations. *Toxicol Appl Pharmacol* **122:** 222-232.

Edwards JR, Marty MS and Atchison WD (2005) Comparative sensitivity of rat cerebellar neurons to dysregulation of divalent cation homeostasis and cytotoxicity caused by methylmercury. *Toxicol Appl Pharmacol* **208:** 222-232.

Eilers L, Callewaert G, Armstrong C and Konnerth A (1995) Calcium signaling in a narrow somatic submembrane shell during synaptic activity in cerebellar Purkinje neurons. *Proc Natl Acad Sci USA* **92:** 10272-10276.

Hare MF and Atchison WD (1995) Methylmercury mobilizes Ca^{2+} from intracellular stores sensitive to inositol 1,4,5-trisphosphate in NG108-15 cells. *J Pharmacol Exp Ther* **272:** 1016-1023.

Hare MF, McGinnis KM and Atchison WD (1993) Methylmercury increases intracellular concentrations of Ca^{2+} and heavy metals in NG108-15 cells. *J Pharmacol Exp Ther* **266:** 1626-1635.

Hunter D and Russell DS (1954) Focal cerebellar atrophy in human subject due to organic mercury compounds. *J Neurol Neurosurg Psych* **17:** 235-241.

Juang MS (1976) An electrophysiological study of the action of methylmercuric chloride and mercuric chloride on the sciatic nerve-sartorius muscle preparation of the frog. *Toxicol Appl Pharmacol* **37:** 339-348.

Juang MS and Yonemura K (1975) Increased spontaneous transmitter release from presynaptic nerve terminal by methylmercuric chloride. *Nature* **256:** 211-213.

Kauppinen RA, Komulainen H and Taipale H (1989) Cellular mechanisms underlying the increase in cytosolic free calcium concentration induced by methylmercury in cerebrocortical synaptosomes from guinea pig. *J Pharmacol Exp Ther* **248:** 1248-1254.

Komulainen H and Bondy SC (1987) Increased free intrasynaptosomal Ca^{2+} by neurotoxic organometals: distinctive mechanism. *Toxicol Appl Pharmacol* **88:** 77-86.

Konnerth A, Dreessen J and Augustine GJ (1992) Brief dendritic calcium signals initiate long-lasting synaptic depression in cerebellar Purkinje cells. *Proc Nat Acad Sci USA* **89:** 7051-7055.

Leyshon-Borland K, Jasani B, Morgan AJ (1994) The localization of mercury and metallothionein in the cerebellum of rats experimentally exposed to methylmercury. *Histochem J* **26:** 161-169.

Limke TL and Atchison WD (2002) Acute exposure to methylmercury opens the mitochondrial permeability transition pore in rat cerebellar granule cells. *Toxicol Appl Pharmacol* **178:** 52-61.

Limke TL, Otero-Montãnez JK and Atchison WD (2003) Evidence for interactions between intracellular stores during methylmercury-induced intracellular calcium dysregulation in rat cerebellar granule neurons. *J Pharmacol Exp Ther* **304:** 948-958.

Limke TL, Heidemann SR and Atchison (2004) Disruption of intraneuronal divalent cation regulation by methylmercury: are specific targets involved in altered neuronal development and cytotoxicity in methylmercury poisoning? *NeuroToxicology* **25:** 741-760.

Llinas R and Nicholson C (1975) Calcium role in depolarization-secretion coupling: an aequorin study in squid giant synapse. *Proc Natl Acad Sci U S A* **72:**187-190.

Marty MS and Atchison WD (1997) Pathways mediating Ca^{2+} entry in rat cerebellar granule cells following in vitro exposure to methylmercury. *Toxicol Appl Pharmacol* **147:** 319-330.

Marty MS and Atchison WD (1998) Elevation of intracellular Ca^{2+} as a probable contributor to decreased viability in cerebellar granule cells following acute exposure to methylmercury. *Toxicol Appl Pharmacol* **150:** 98-105.

Minnema DJ, Cooper GP and Greenland RD (1989) Effects of methylmercury on neurotransmitter release from rat brain synaptosomes. *Toxicol Appl Pharmacol* **99:** 510-521.

Miyakawa H, Lev-Ram V, Lasser-Ross, N and Ross WN (1992) Calcium transients evoked by climbing fiber and parallel fiber synaptic inputs in guinea pig cerebellar Purkinje neurons. *J Neurophysiol* **68:** 1178-1189.

O'Kusky J (1985) Synaptic degeneration in rat visual cortex after neonatal administration of methylmercury. *Exp Neurol* **89:** 32-47.

O'Kusky JR and McGeer EG (1985) Methylmercury poisoning of the developing nervous

system in the rat; decreased activity of glutamic acid decarboxylase in cerebral cortex and neostriatum. *Develop Brain Res* **2:** 299-306.

O'Kusky JR, Radke JM and Vincent SR (1988) Methylmercury-induced movement and postural disorders in developing rat: loss of somatostatin-immunoreactive interneurons in the striatum. *Develop Brain Res* **40:** 11-23.

Otis TS and Mody I (1992) Modulation of decay kinetics and frequency of $GABA_A$ receptor-mediated spontaneous inhibitory postsynaptic currents in hippocampal neurons. *Neuroscience* **49:** 13-32.

Ross WN and Werman R (1987) Mapping calcium transients in the dendrites of Purkinje cells from the guinea-pig cerebellum in vitro. *J Physiol (Lond)* **389:** 319-336

Rusakov DA (2006) Ca^{2+}-dependent mechanisms of presynaptic control at central synapses. *Neuroscientist* **4**: 317-326.

Savič N and Sciancalepore M (1998) Intracellular calcium stores modulate miniature GABA-mediated synaptic currents in neonatal rat hippocampal neurons. *Eur J Neurosci* **10:** 3379-3386.

Shigematsu J, Yasuda T, Goto Y, Tanaka K and Tobimatsu S (2000) Chronic effects of methylmercury on the cerebral function in rats. *J Neurol Sci* **182:** 69-75.

Stuart GJ, Dolt H-U and Sakmann B (1993) Patch-clamp recordings from the soma and dendrites of neurons in brain slices using infrared video microscopy. *Pflügers Arch* **423:** 511-518

Sugimori M and Llinás RR (1990) Real-time imaging of calcium influx in mammalian cerebellar Purkinje cells in vitro. *Proc Natl Acad Sci USA* **87:** 5084-5088.

Tan XX, Tang C, Castoldi AF, Manzo L and Costa LG (1993) Effects of inorganic and organic mercury on intracellular calcium levels in rat T lymphocytes. *J Toxicol Environ Health* **38:**159-170.

Tank DW, Sugimori M, Conner JA and Llinás RR (1988) Spatially resolved calcium dynamics of mammalian Purkinje cells in cerebellar slice. *Science* **242:** 773-777.

Takeuchi T, Matsumoto H, Sasaki M, Kambara T, Shiraishi Y, Hirata Y, Nobukiro M and Satoh H (1968) Pathology of Minamata disease. *Kumamoto Med J* **34:** 521-524.

Yuan Y and Atchison WD (1993) Disruption by methylmercury of membrane excitability and synaptic transmission of CA1 neurons in hippocampal slices of the rat. *Toxicol Appl Pharmacol* **120:** 203-215.

Yuan Y and Atchison WD (1995) Methylmercury acts at multiple sites to block hippocampal synaptic transmission. *J Pharmacol Exp Ther* **275:** 1308-1316.

Yuan Y and Atchison WD (1997) Action of methylmercury on $GABA_A$ receptor-mediated inhibition is primarily responsible for its early stimulatory effects on hippocampal CA1 synaptic transmission. *J Pharmacol Exp Ther* **282:** 64-73.

Yuan Y and Atchison WD (1999) Comparative effects of methylmercury on parallel-fiber and climbing-fiber response of rat cerebellar slices. *J Pharmacol Exp Ther* **288:** 1015-1025.

Yuan Y and Atchison WD (2003) Methylmercury differentially affects $GABA_A$ receptor-mediated spontaneous IPSCs in Purkinje and granule cells of rat cerebellar slices. *J Physiol (Lond.)* **550:** 191-204.

Yuan Y and Atchison WD (2005) Methylmercury induces a spontaneous, transient slow inward chloride current in Purkinje cells of rat cerebellar slices. *J Pharmacol Exp Ther* **313:** 751-764.

Yuan Y, Otero-Montañez JKL, Yao A, Herden CJ, Sirois JE and Atchison, WD (2005) Inwardly rectifying and voltage-gated outward potassium channels exhibit low sensitivity to methylmercury. *NeuroToxicology* **26**: 439-454.

Molecular Pharmacology Fast Forward. Published on January 23, 2007 as DOI: 10.1124/mol.106.031286
This article has not been copyedited and formatted. The final version may differ from this version.

FOOTNOTES

Supported by NIH grants R01-ES03299 and R01-ES11662. The Leica Confocal microscope was purchased with funds provided by the Michigan Life Sciences Corridor Grant Program of the State of Michigan Economic Development Corporation.

Molecular Pharmacology Fast Forward. Published on January 23, 2007 as DOI: 10.1124/mol.106.031286
This article has not been copyedited and formatted. The final version may differ from this version.

FIGURE LEGENDS

Figure 1. MeHg causes a biphasic effect on frequency and amplitude of sEPSCs of cerebellar Purkinje cells. *A-G*, depicts a representative time course of effect of 20 μM MeHg on sEPSCs of a Purkinje cell in an isolated cerebellar slice. Whole cell sEPSCs were recorded from a Purkinje cell in a sagittal cerebellar slice at a holding potential (HP) of -70 mV in the presence of 10 μM bicuculline in the external solution to block $GABA_A$ receptor-mediated sIPSCs. Data are shown before (Control) and at selected time points after MeHg exposure. *H*, Cumulative distribution of inter-sEPSC intervals during the initial 25 min of MeHg exposure. a, control; b, MeHg 5 min; c, MeHg 10 min; d, MeHg 25 min. MeHg shifted the curve of the cumulative inter-event intervals distribution to the left during the first 25 min MeHg exposure. Each trace is a representative depiction of 13 individual experiments.

Figure 2. MeHg causes a biphasic effect on frequency of sEPSCs or sIPSCs of cerebellar Purkinje cells in a concentration- and time-dependent manner. *A*, Time courses of effects of 10 - 100 μM MeHg on sEPSC frequency. *B*, Time courses of concentration-dependent effects of 10 - 100 μM MeHg on frequency of sIPSCs of cerebellar Purkinje cells in slices. In both cases, MeHg was applied at time = 0 min. Data were sampled over 2 min periods and each time point represents the average of spontaneous sIPSCs for that 2 min block. Data collected before MeHg treatment (at 0 min) serve as the control and data collected during MeHg exposure are normalized to the value of the control. All values are the mean ± SEM of 5 -13 (*A*) and 7 -10 (B) individual experiments, respectively.

Molecular Pharmacology Fast Forward. Published on January 23, 2007 as DOI: 10.1124/mol.106.031286
This article has not been copyedited and formatted. The final version may differ from this version.

Figure 3. MeHg increases Fluo-4 fluorescence intensity in the molecular layer, granule cell layer, dendrites of Purkinje cells, but not Purkinje cell soma in cerebellar slices. The cerebellar slices were preloaded with Fluo-4/AM for 60 min at room temperature and were washed thoroughly before recording. Pseudocolor confocal images of Ca^{2+}-induced Fluo-4 fluorescence in the molecular layer (ML), Purkinje cell layer (PCL) and granule cell layer (GCL) of a representative sagittal (Top panel) or a transverse (Bottom panel) cerebellar slice were taken before (Control) and at different time points during exposure to 10 or 20 μM MeHg, respectively. Increased $[Ca^{2+}]_i$ is denoted by yellow and white pseudocolor. Blue color indicates a very high $[Ca^{2+}]_i$ that exceeds the sensitivity range of Fluo-4. The same is true for all subsequent figures. Each time point is representative of 4 - 10 individual experiments. The bottom pseudocolor bar indicates the Fluo-4 fluorescence intensity scale.

Figure 4. MeHg causes an increase in Fluo-4 fluorescence in the dendrites and in the subplasmalemmal shell, but not the soma of Purkinje cells in the molecular layer of cerebellar slices. Pseudocolor representation of confocal images of Ca^{2+}-induced Fluo-4 fluorescence in Purkinje cell dendrites in the inner part of the molecular layer of a sagittal cerebellar slice (Top panel) or in Purkinje cell soma regions of another sagittal cerebellar slice (Bottom pannel) were taken before (Control) and at different time points during 100 or 20 μM MeHg exposure, respectively. Changes in fluorescence intensity in the dendrites or subplasmalemmal shell are indicated by arrows. Each image is a representative depiction of 5 - 7 individual experiments.

Figure 5. Times to MeHg-induced maximum increase in frequency of spontaneous postsynaptic currents and Fluo-4 fluorescence intensity are similar. *A* and *C*, Comparison of time courses of effects of 20 (*A*) and 100 μM MeHg (*C*) on Fluo-4 fluorescence intensity measured in the molecular layer (ML) and granule cell layer (GCL). Data collected during MeHg exposure are normalized to that of the MeHg-pretreatment control. Each point is the mean ± SEM of 7 - 9 individual experiments. *B* and *D*, Comparison of mean times to maximum increase in Fluo-4 fluorescence measured in the molecular layer and the frequency of sIPSCs recorded from Purkinje cell soma after exposure to 20 (*B*) and 100 μM MeHg (*D*). Data are the mean ± SEM of 7 - 10 individual experiments.

Figure 6. Times to onset of changes in Fluo-4 fluorescence signals in the molecular layer and the frequency of sIPSCs appear to be correlated. *S*imultaneous recordings of changes in Fluo-4 fluorescence the molecular layer and sIPSCs in a Purkinje cell were carried out in the same cerebellar slice. *Left*, Time course of effect of 20 μM MeHg on Fluo-4 fluorescence intensity in the molecular layer of a sagittal cerebellar slice. *Right*, Time courses of effect of 20 μM MeHg on sIPSCs recorded from a Purkinje cell in the same cerebellar slice as on the left. Each image or current trace is a representative depiction of 6 individual experiments.

Figure 7. Changes in Fluo-4 fluorescence signals in the granule cell and molecular layers including the Purkinje cell dendrites appear to correlate with changes in sIPSC frequency. *S*imultaneous recordings of changes in Fluo-4 fluorescence in the molecular layer and sIPSCs in a Purkinje cell were carried out in the same cerebellar slice. *Left*, Time-course of effect of 20

μM MeHg on sIPSCs recorded from a Purkinje cell in a sagittal cerebellar slice. *Right*, Comparison of changes induced by 20 μM MeHg in Fluo-4 fluorescence intensity in the molecular and granule cell layers of the same sagittal cerebellar slice as shown at the left. Note the shadows of a recording electrode were seen over the molecular layer in each image. Each image or current trace is a representative depiction of 6 individual experiments.

Figure 8. BAPTA pretreatment suppresses MeHg-induced initial increase in sIPSC frequency of Purkinje cells in cerebellar slices. *A-H*, Samples of continuous recordings of sIPSCs from a representative Purkinje cell in cerebellar slice before (*A*), after 30 min incubation of 50 μM BAPTA (*B*) and at different time points after exposure to 20 μM MeHg plus 50 μM BAPTA/AM (*C-H*, n = 7), respectively. *I*, Time courses of effects of 20 and 100 μM MeHg on sIPSC frequency. After 30 min of BAPTA incubation, MeHg was applied at time = 0 min in the continuous presence of 50 μM BAPTA in bath. Data were sampled over a 2 - min period and each time point represents the average of spontaneous sIPSCs for that 2 min block. Data collected before BAPTA treatment (at -30 min) serve as the control and data collected during MeHg exposure are normalized to the control. All values are the mean ± SEM of 6 - 7 individual experiments.

Table 1. Comparison of times to MeHg-induced peak increase in frequency and times to complete block of sEPSCs and sIPSCs in Purkinje cells in cerebellar slices.

MeHg (μM)	sEPSCs		sIPSCs	
	Time to P-F (min)[a]	Time to Block (min)[b]	Time to P-F (min)[a]	Time to Block (min)[b]
10	37.5 ± 4.8 (6)[c]	115.0 ± 5.0 (4)	30.0 ± 6.1 (7)	96.0 ± 10.4 (5)
20	24.6 ± 4.0 (13)	66.1 ± 4.8 (9)	20.0 ± 2.2 (12)	60.0 ± 4.0 (9)
100	6.7 ± 0.8 (11)	17.6 ± 1.3 (9)	6.8 ± 0.5 (10)	16.4 ± 1.0 (10)

[a] Time to onset of peak increase in sEPSC or sIPSC frequency (P-F).

[b] Time to complete cessation of sEPSCs or sIPSCs.

[c] Mean ± SEM (n).

Fig. 1

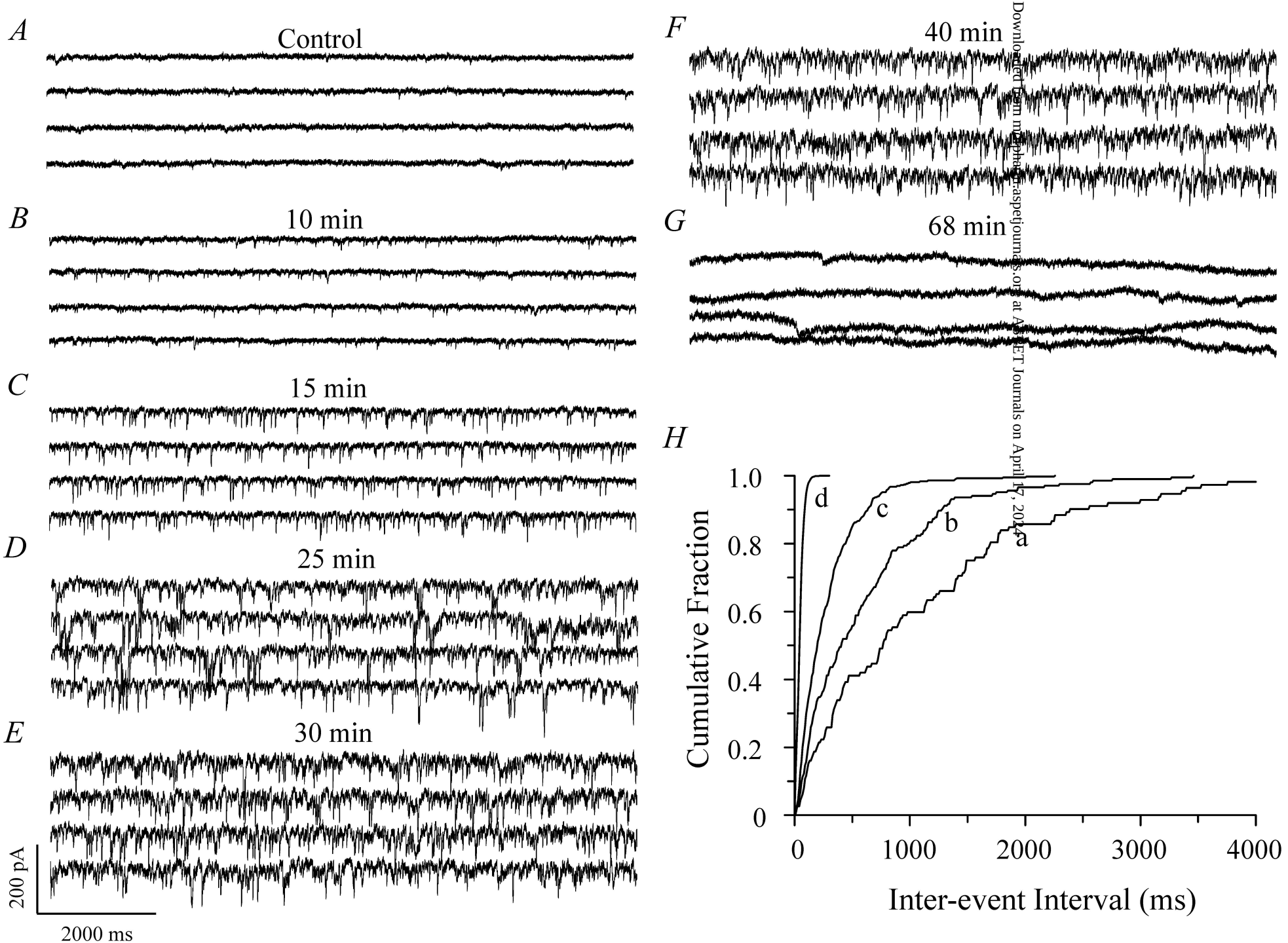

Fig. 2

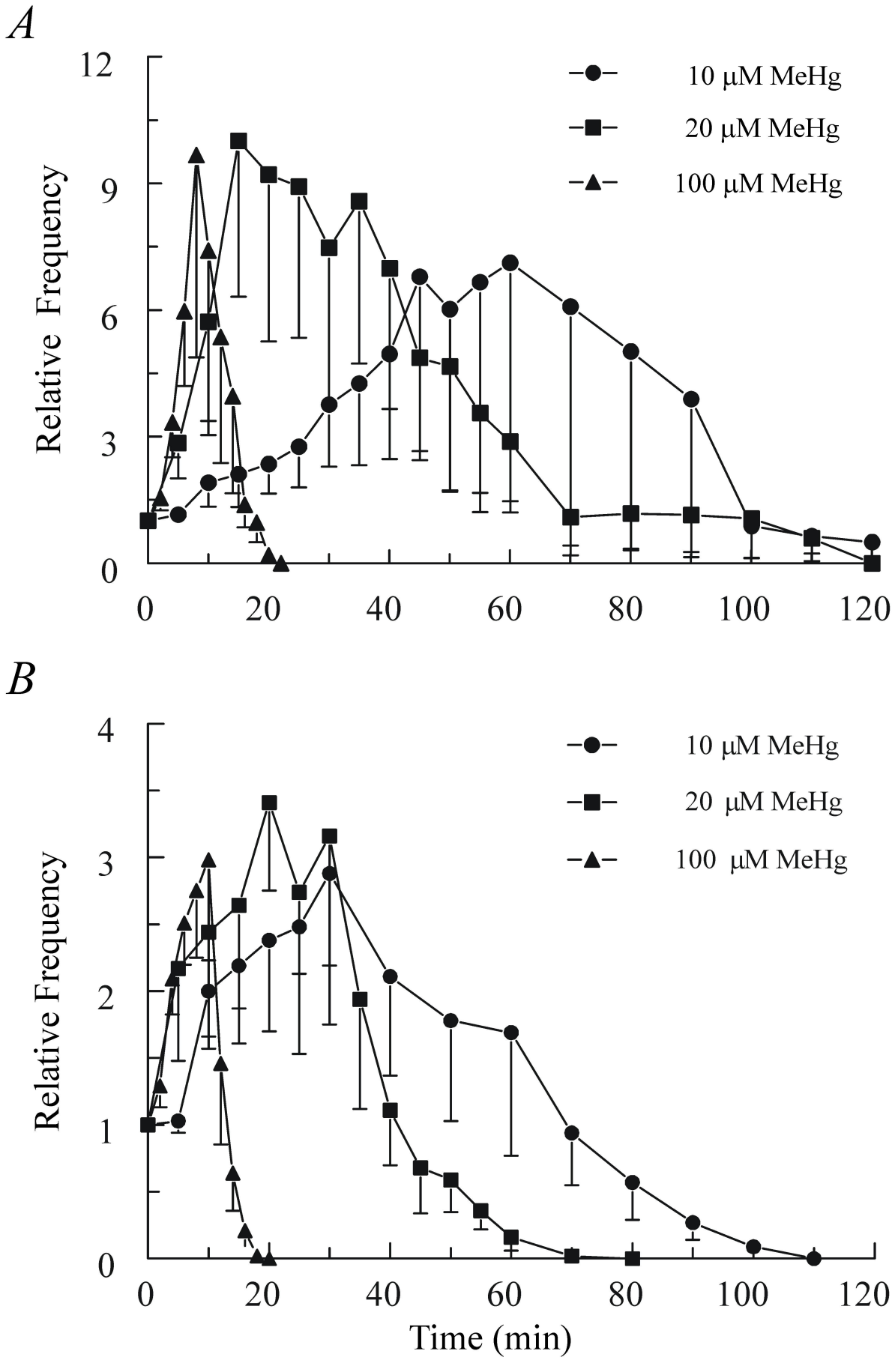
A
12
9
6
3
0
Relative Frequency
10 μM MeHg
20 μM MeHg
100 μM MeHg
0
20
40
60
80
100
120
B
4
3
2
1
0
Relative Frequency
10 μM MeHg
20 μM MeHg
100 μM MeHg
0
20
40
60
80
100
120
Time (min)

Fig. 3

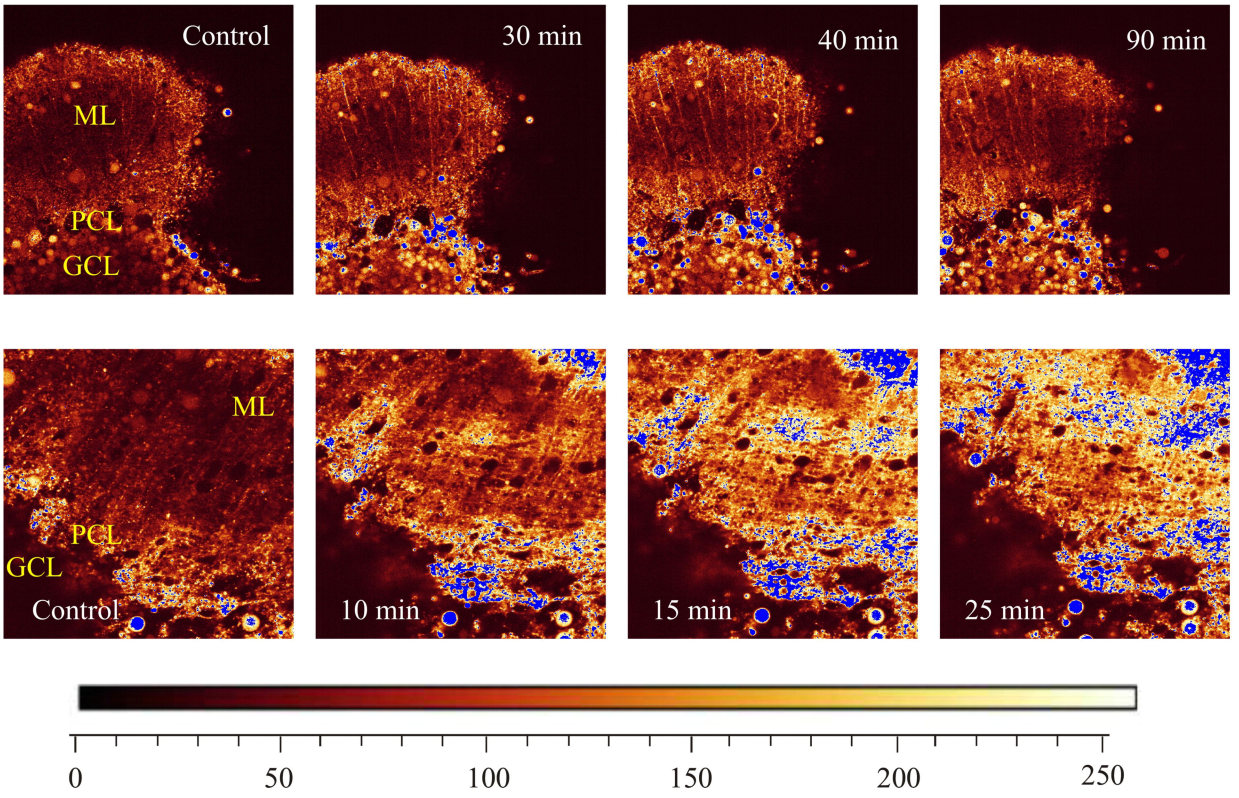
Control
30 min
40 min
90 min
ML
PCL
GCL
ML
PCL
GCL
Control
10 min
15 min
25 min
0
50
100
150
200
250

Fig. 4

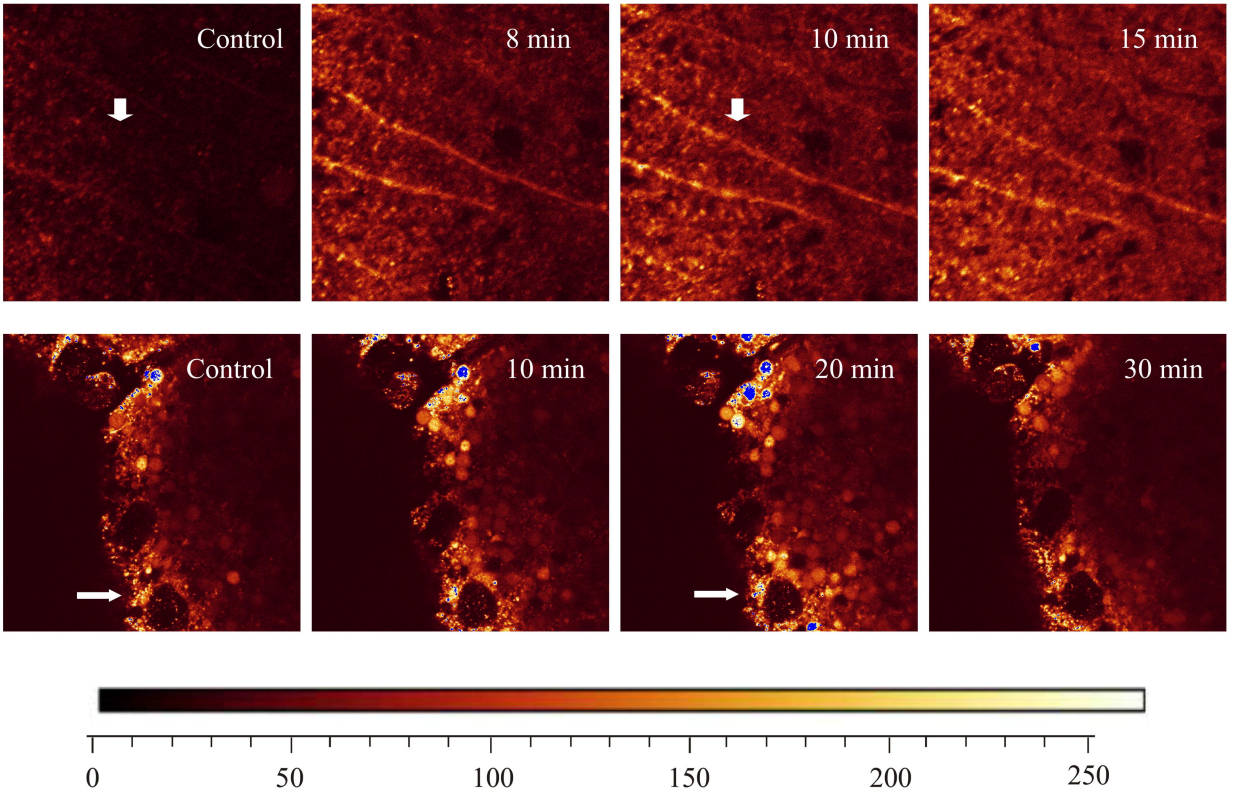
Control
8 min
10 min
15 min
Control
10 min
20 min
30 min
0
50
100
150
200
250

Fig 5

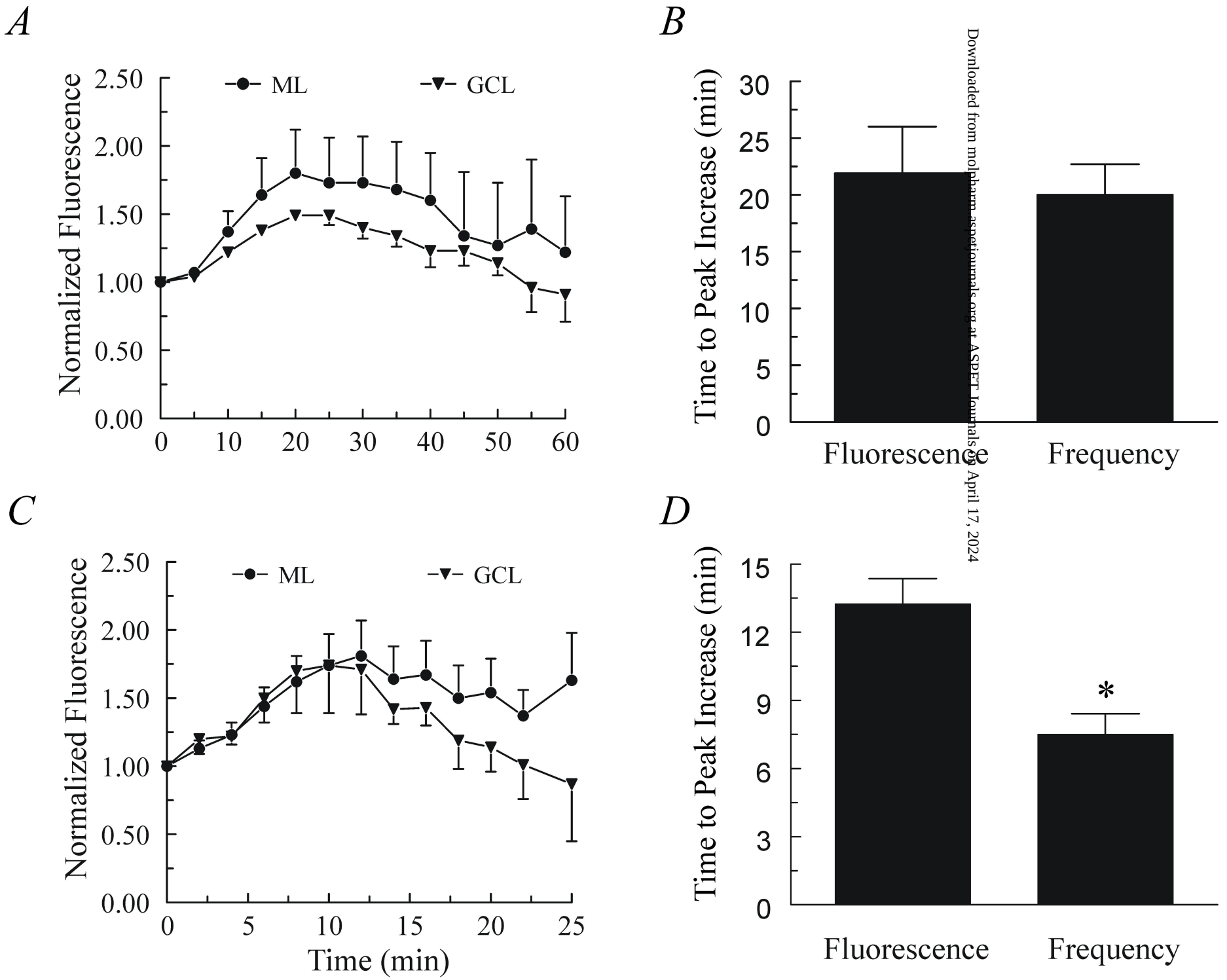

Fig. 6

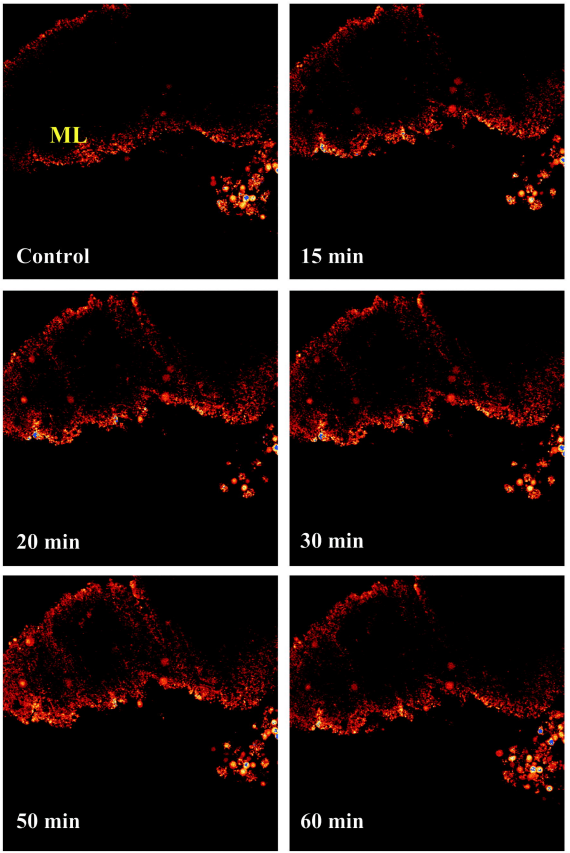
ML
Control
15 min
20 min
30 min
50 min
60 min

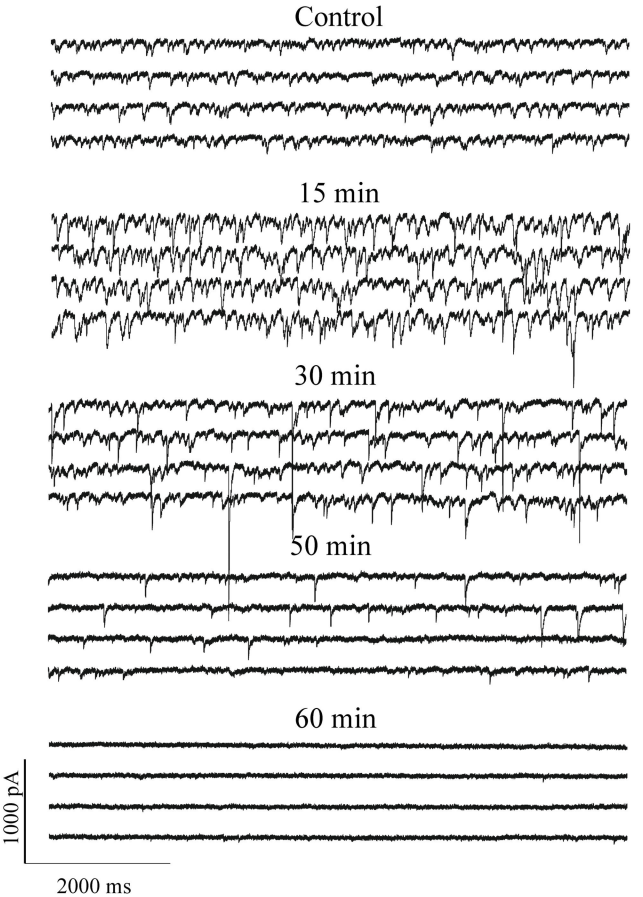
Control
15 min
30 min
50 min
60 min
1000 pA
2000 ms

Fig. 7

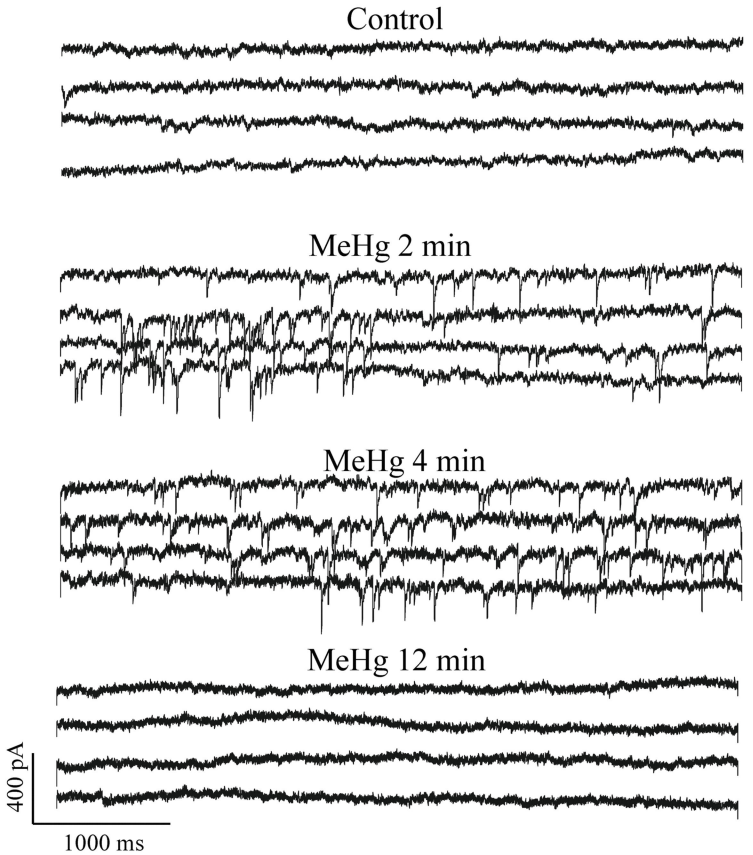
Control
MeHg 2 min
MeHg 4 min
MeHg 12 min
400 pA
1000 ms

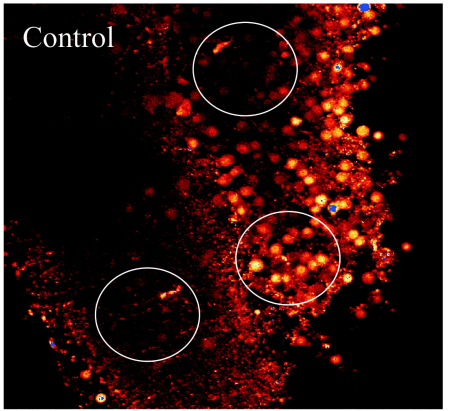
Control

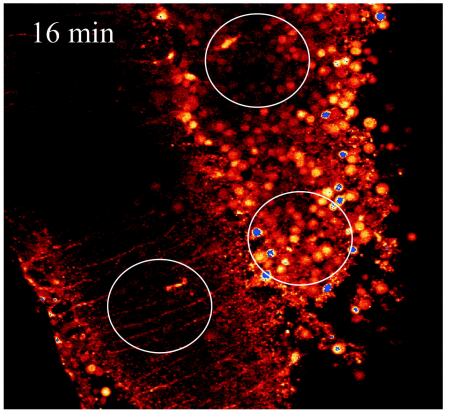
16 min

Fig. 8